

Unsupervised Feature Learning by Cross-Level Instance-Group Discrimination

Xudong Wang
UC Berkeley / ICSI

xdwang@eecs.berkeley.edu

Ziwei Liu
S-Lab, NTU

ziwei.liu@ntu.edu.sg

Stella X. Yu
UC Berkeley / ICSI

stellayu@berkeley.edu

Abstract

Unsupervised feature learning has made great strides with contrastive learning based on instance discrimination and invariant mapping, as benchmarked on curated class-balanced datasets. However, natural data could be highly correlated and long-tail distributed. Natural between-instance similarity conflicts with the presumed instance distinction, causing unstable training and poor performance.

Our idea is to discover and integrate between-instance similarity into contrastive learning, not directly by instance grouping, but by cross-level discrimination (CLD) between instances and local instance groups. While invariant mapping of each instance is imposed by attraction within its augmented views, between-instance similarity could emerge from common repulsion against instance groups.

Our batch-wise and cross-view comparisons also greatly improve the positive/negative sample ratio of contrastive learning and achieve better invariant mapping. To effect both grouping and discrimination objectives, we impose them on features separately derived from a shared representation. In addition, we propose normalized projection heads and unsupervised hyper-parameter tuning for the first time.

Our extensive experimentation demonstrates that CLD is a lean and powerful add-on to existing methods such as NPID, MoCo, InfoMin, and BYOL on highly correlated, long-tail, or balanced datasets. It not only achieves new state-of-the-art on self-supervision, semi-supervision, and transfer learning benchmarks, but also beats MoCo v2 and SimCLR on every reported performance attained with a much larger compute. CLD effectively brings unsupervised learning closer to natural data and real-world applications. Our code is publicly available at: <https://github.com/frank-xwang/CLD-UnsupervisedLearning>.

1. Introduction

Representation learning aims to extract latent or semantic information from raw data. Typically, a model is first trained on a large-scale annotated dataset [37] and then tuned on a small-scale dataset for a downstream task [27]. As the

model gets bigger and deeper [28, 31], more annotated data are needed; supervised pre-training is no longer viable.

Self-supervised learning [15, 47, 70, 44, 16, 42] gets around labeling with a pre-text task which does not require annotations and yet would be better accomplished with semantics. For example, to predict the color of an object from its grayscale image does not require labeling; however, doing it well would require a sense of what the object is. The biggest drawback is that pre-text tasks are domain-specific and hand-designed, and they are not directly related to downstream semantic classification.

Unsupervised contrastive learning has emerged as a direct winning alternative [58, 71, 63, 7, 26]. The training objective and the downstream classification are aligned on discrimination, albeit at different levels of granularities: training is to discriminate known individual instances, whereas testing is to discriminate unknown groups of instances.

Contrastive learning approaches have made great strides with two ideas: invariant mapping [25] and instance discrimination [58]. That is, the learned representation should be 1) stable for certain transformed versions of an instance, and 2) distinctive for different instances. Both aspects can be formulated without labels, and the feature learned appears to automatically capture semantic similarity, as benchmarked by downstream classification on standard datasets such as CIFAR100 and ImageNet [7]. However, these datasets are curated with distinctive and class-balanced instances, whereas natural data could be highly correlated within the class (e.g., repeats) and long-tail distributed across classes.

Natural between-instance similarity demands instance grouping not instance discrimination, where *all the instances are presumed different*. Consequently, feature learning by instance discrimination is unstable and under-performing without instance grouping, whereas instance grouping based on the feature learned without instance discrimination is easily trapped into degeneracy. Ad-hoc tricks [4, 5] and mutual information maximization with a uniform class distribution prior [34] have been used to prevent feature degeneracy.

We propose to discover and integrate between-instance similarity into contrastive learning, not directly by instance grouping, e.g., by imposing group-level discrimination as

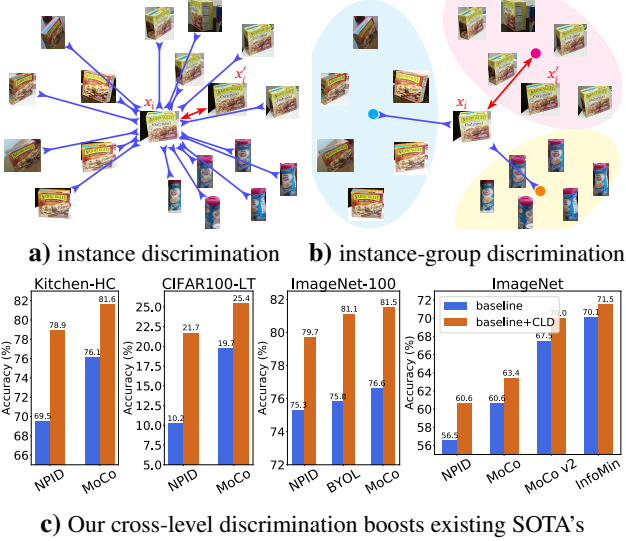


Figure 1: Our unsupervised feature learning discovers similar instances and integrates grouping into instance-level discrimination, outperforming the state-of-the-art (SOTA) classifiers on highly correlated, long-tail, or balanced datasets. **a)** Instance discrimination presumes all instances distinctive: Instance x_i **attracts** (\leftrightarrow) its augmented version x'_i and **repels** (\times) all other instances including those highly similar ones. **b)** We propose cross-level discrimination (CLD) between instance x_i and local groups of alternative views $\{x'_j\}$. x_i **attracts** (\leftrightarrow) the group centroid that x'_i belongs to and **repels** (\times) other group centroids. Visually similar instances tend to attract/repel the same group centroids and are thus mapped closer. **c)** Our CLD can be added to existing methods such as NPID [58], MoCo [26], MoCo v2 [8], InfoMin [54] and BYOL [23]. It consistently provides a significant performance boost on highly correlated (HC), long-tail (LT), and standard balanced ImageNet datasets.

DeepCluster [4, 5] or by regulating instance-level discrimination based on the grouping outcome as Local Aggregation (LA) [71], but by imposing cross-level discrimination (CLD) between instances and local instance groups.

Contrastive learning is built upon dual forces of attraction and repulsion [25]. Existing methods generally assume repulsion between different instances and attraction within *known groupings* of instances, e.g., between augmented views of the same data instances [58, 71, 26], or between data captured from different times, views, or modalities of the same physical instances [45, 1, 55, 53].

Feature learning with between-instance similarity calls for attraction within *unknown groupings*, not the universal between-instance repulsion (Fig. 1a). A chicken-and-egg challenge is to discover such groupings for feature learning while the feature for the groupings is still to be developed.

Our key insight is that grouping could result from not just attraction, but also common repulsion. While invariant map-

ping is achieved by within-instance similarity from attraction across augmented views, between-instance similarity can emerge from repulsion against common instance groups, the centroids of which are more stable in the developing feature space. That is, to discover the most discriminative feature that also respects natural instance grouping, we desire each instance to attract the closest group related by augmentation and repel groups of other instances that are far from it.

In our approach (Fig. 1b), between-instance similarity, unknown *a priori*, is not captured directly as attraction between instances, but by more likely common attraction and repulsion between each instance and instance group centroids. By pulling an instance towards and pushing it against more stable instance groups, *similar* instances get mapped closer in the feature space. To effect both grouping and discrimination objectives on feature learning, we also impose them on features separately derived from a shared representation.

Such an interplay between attraction and repulsion has been utilized to model perceptual popout [65, 2], as well as simultaneous image segmentation and depth segregation [64, 41]. However, those works are prior to deep learning and aim at grouping pixels based on certain fixed pixel-level feature such as edges, whereas our work aims at learning the image-level feature discriminatively.

We add CLD to popular state-of-the-art (SOTA) unsupervised feature learning approaches (Fig. 1c), e.g., NPID [58], MoCo [26], InfoMin [54] (all three based on instance discrimination), and BYOL [23] (focusing only on invariant mapping without instance discrimination). CLD delivers a significant performance boost not only on highly correlated, long-tail, and balanced datasets, but also on all the self-supervision, semi-supervision, and transfer learning benchmarks under fair comparison settings [58, 26, 69].

Our work makes three major contributions. **1)** We extend unsupervised feature learning to natural data with high correlation and long-tail distributions. **2)** We propose cross-level discrimination between instances and local groups, to discover and integrate between-instance similarity into contrastive learning. We also propose normalized projection heads and unsupervised hyper-parameter tuning. **3)** Our experimentation demonstrates that adding CLD to existing methods has a negligible overhead and yet delivers a significant boost. It achieves new SOTA on all the benchmarks, and beats MoCo v2 [8] and SimCLR [7] on every reported performance attained with a much larger compute.

2. Related Works

Unsupervised representation learning [15, 47, 70, 44, 16, 38, 33, 21, 68] aims to learn features transferable to downstream tasks. Our work is closely related to contrastive learning and unsupervised feature learning with grouping.

Contrastive learning maps positive samples closer and negative samples apart in the feature space [58, 42, 53, 26, 8, 7].

Positive samples come from augmented views of each instance, whereas negative ones come from different instances. The key distinction among existing methods lies in how these samples are obtained and maintained during learning.

Batch methods [7] draw samples from the current mini-batch with the same encoder, updated end-to-end with back-propagation. **Memory-bank methods** [58, 42] draw samples from a memory bank that stores the prototypes of all the instances computed previously. **Hybrid methods** [26, 8] encode positive samples by a momentum-updated encoder and maintain negative samples in a queue.

Instance discrimination methods presume distinctive instances. Their performance drops on natural data that are highly correlated or long-tail distributed, e.g., consecutive frames in a video, or different views of the same instance. Note that our setting is *completely unsupervised* and different from learning representation across views [1, 55, 53]: We have mixed data without any object or view labels.

Feature learning with grouping exploits natural organization of data [59, 60, 5, 71]. Unlike self-supervised learning [47, 44, 21], it does not require domain knowledge [4].

Earlier works restrict learning to linear feature transformations. DisCluster [11, 14] and DisKmeans [62] iteratively apply K-means to generate cluster labels and then use linear discriminant analysis (LDA) to select the most discriminative subspace. [61] applies LDA along with spectral clustering [57]. [43] uses linear regression as a regularization term to handle out-of-sample data in spectral clustering.

Nonlinear feature transformations have also been studied. [52] applies a deep sparse autoencoder to a normalized graph similarity matrix and performs K-means on the latent representation. [56] implements t-SNE embedding with a deep neural network. Deep Embedded Clustering [59] simultaneously learns cluster centroids and feature mapping such that centroid-based soft assignments in the embedding matches a desirable target distribution.

Recent works jointly optimize the feature and the cluster assignment. **DeepCluster** [4, 5] gets pseudo-class labels from global clustering and applies supervised learning to iteratively fine-tune the model, whereas our CLD incorporates local clustering into contrastive metric learning. **Local Aggregation (LA)** [71] identifies a local neighbourhood of each instance through clustering, and restricts instance-level discrimination within individual neighbourhoods, whereas CLD looks beyond local neighbourhoods and conducts cross-level instance-group discrimination. **PCL** [39] is a concurrent work that compares instance features with group centroids which are obtained through global clustering per epoch, whereas our CLD uses local clustering per batch and compares instance-group features within the batch. Global clusters not only takes more time to compute during training, but conceptually also do not align with classes in downstream tasks. Empirically, PCL gains much over MoCo but

not over MoCo v2 [39]. **SegSort** [32] extends representation learning from classification to segmentation. It learns a feature per pixel, and assumes that all the pixels in the same region form a cluster in the feature space. SegSort uses *one* common feature and contrasts each *pixel* with cluster centroids in the feature from the *same*-view, whereas our CLD uses *two* separate features and contrasts each *image* with cluster centroids in the feature from a *different* view.

Discussions. While clustering on a fixed feature is well studied [19], clustering with an adapting feature is a tricky model selection problem: **1)** Clustering could fall into trivial solutions where most samples are assigned to a single cluster, trapping feature learning into degeneracy [4]. **2)** Without any external supervision, it is unclear how to ensure that the learned feature captures latent semantics.

Our work combines contrastive learning and grouping in a single framework, by expanding discrimination between instances to that between instances and local groups. Discrimination prevents feature learning from degeneracy, while grouping improves stability and helps instance-level discrimination see beyond the finest granularity. With these two aspects integrated, our CLD significantly improves the learned representation for downstream classification.

3. Learning with Cross-Level Discrimination

Given n images, we regard instance x_i as a *view* obtained by a certain transformation (e.g. cropping) of the i -th image. Let x_i and x'_i denote two different *views* of the i -th instance. **Contrastive learning** [25, 58, 26, 53, 45, 7] aims to learn a mapping function f such that in the $f(x)$ feature space, instance x_i is **1)** close to positive sample x'_i (**invariant mapping**), and **2)** far from negative sample x_j (with $j \neq i$) of any other instances (**instance discrimination**).

We model f by a convolutional neural network (CNN) with parameters θ , mapping x onto a d -dimensional hypersphere such that $\|f(x)\| = 1$. Let f, f^+, f^- denote the feature for an instance and its positive / negative samples respectively. We optimize θ by minimizing loss C over all n instances so that f attracts f^+ and repels f^- .

instance-centric contrastive loss:

$$C(f_i, f_i^+, f_{\neq i}^-) = -\log \frac{\exp \frac{\langle f_i, f_i^+ \rangle}{T}}{\exp \frac{\langle f_i, f_i^+ \rangle}{T} + \sum_{j \neq i} \exp \frac{\langle f_i, f_j^- \rangle}{T}} \quad (1)$$

Temperature T is a hyperparameter regulating what distance is close. C is the noise contrastive estimation (NCE) [24] of softmax instance classification loss [58], and it can be viewed as maximizing a lower bound of mutual information (MI) between samples of the same instances [46, 25, 45].

Implementation of $(f_i, f_i^+, f_{\neq i}^-)$ during training. For sample x_i , the self feature is $f_i = f(x_i)$, whereas positive feature f_i^+ and negative feature $f_{\neq i}^-$ come from a memory bank v that holds the representative feature for $\{x_i\}_{i=1}^n$. It

5. Cross-view comparisons between x_i and x'_i focus the model more on invariant mapping.

Probabilistic interpretation of CLD. Our CLD objective can be understood as minimizing the cross entropy between hard clustering assignment p_{ij} (as *ground-truth*) based on $f_G(x_i)$ and soft assignment q_{ij} predicted from $f_G(x'_i)$ in a different view. Since $p_{ij} = 1$ only when $j = \Gamma(i)$, we have a loss that validates local groupings across different views:

$$-E_p[\log q] = \sum_i C(f_G(x'_i), M_{\Gamma(i)}, M_{\neq\Gamma(i)}; T_G). \quad (2)$$

Total contrastive learning loss. We add CLD to instance discrimination (with temperatures T_I, T_G , weight λ) in symmetrical terms over views x_i and x'_i :

$$L(f; T_I, T_G, \lambda) = \underbrace{\sum_i C(f_I(x_i), v_i, v_{\neq i}; T_I) + C(f_I(x'_i), v_i, v_{\neq i}; T_I)}_{\text{instance-level discrimination}} + \lambda \underbrace{\sum_i C(f_G(x'_i), M_{\Gamma(i)}, M_{\neq\Gamma(i)}; T_G) + C(f_G(x_i), M'_{\Gamma(i)}, M'_{\neq\Gamma(i)}; T_G)}_{\text{cross-level discrimination}}$$

We analyze why two feature branches are better than one branch, where $f_I = f_G$ and M is simply the group centroids of $f_I(x_i)$ or v . In that case, while the instance discrimination term would repel x_i against any other instances $\{x_j\}$, the CLD term would make x_i attract *some other* instances $\{x_j\}$ in the same group of x_i through their group centroid. Minimizing the two terms would lead to opposite effects no matter what the local clustering is. Basing instance feature f_I and group feature f_G as separate branches off feature f would force f to be discriminative enough for the instance branch yet loosely similar enough for the group branch.

Normalized projection head. Existing methods derive instance feature $f_I(x)$ by mapping the latent feature $f(x)$ onto a unit hypersphere with first a projection head and then normalization. NPID [58] and MoCo [26] use one FC layer as a linear projection head. MoCo v2 [8], SimCLR [7], and BYOL [23] use a multi-layer perceptron (MLP) head; it is better for large datasets and worse for small datasets.

We propose to normalize both the FC layer weights W and the shared feature vector f so that projecting f onto W simply calculates their cosine similarity. The t -th component of normalized feature $N(x_i)$ (where $N = f_I$ or $N = f_G$) is:

$$N_t(x_i) = \frac{W_t}{\|W_t\|}, \frac{f(x_i)}{\|f(x_i)\|} \cdot \quad (3)$$

Normalized linear (NormLinear) or MLP (NormMLP) projection heads bring additional gains to CLD. Empirically, they help reduce feature variance from data augmentation.

4. Experiments

We use ResNet-50 for ImageNet data and ResNet-18 otherwise. We compare linear classification accuracies on ImageNet, and follow NPID on using kNN accuracies ($k =$

200) for all the small-scale benchmarks. The kNN accuracies are higher and more fitting for metric learning. Results marked by \dagger are obtained with released code.

We consider 3 types of datasets. **1) High-correlation:** Kitchen-HC is constructed by extracting objects in their bounding boxes from the multi-view RGB-D Kitchen dataset [20]. It has 11 categories with highly correlated samples and 20.8K / 4K / 14.4K instances in train / validation / test sets. **2) Long-tail:** CIFAR10-LT, CIFAR100-LT and ImageNet-LT [40]. **3) Major benchmarks:** CIFAR [36], STL10 [10], ImageNet-100 [53], ImageNet [13]. Following [63], we train models on 5K samples in the *train* set and 100K samples in the *unlabeled* set, and test on the *test* set of STL10.

4.1. Benchmarking Results

Results on high-correlation data. Having highly correlated instances breaks the instance discrimination presumption and causes slow or unstable training. Accuracies in Fig. 3 and feature visualization in Fig. 4 indeed show that CLD is much better and fast converging towards a more distinctive feature representation. At Epoch 10, CLD outperforms by 40% (23% vs. 63%). CLD outperforms NPID by 9.4%, when the number of groups used in local clustering is closer to the number of semantic classes in the downstream classification. Likewise, MoCo + CLD outperforms its counterpart MoCo by 5.5%.

Results on long-tailed data. Table 1 shows that CLD outperforms baselines by a large margin on CIFAR10-LT and

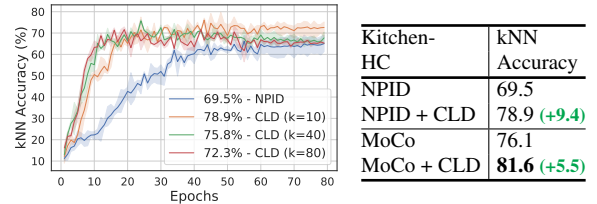


Figure 3: **Left:** CLD is more accurate and fast converging than NPID on Kitchen-HC, esp. when the number of groups is closer to the number of classes 11. The average top-1 kNN accuracy of 5 runs is reported. **Right:** CLD outperforms NPID or MoCo on **high correlation dataset** Kitchen-HC.

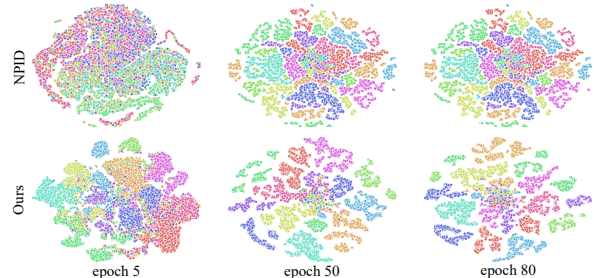


Figure 4: CLD has earlier and better separation between classes (indicated by the dot color) than NPID in the **t-SNE visualization** of instance feature $f_I(x_i)$ on Kitchen-HC.

	CIFAR10-LT		CIFAR100-LT		ImageNet-LT		
	top1	top5	top1	top5	many/med/few	top1	top5
<i>Unsupervised</i>							
NPID [58]	32.3	74.8	10.2	29.8	47.5/21.3/6.6	29.5	51.1
NPID + CLD	41.1	78.9	21.7	44.3	52.4/25.0/8.3	32.7	55.6
vs. baseline	+8.8	+4.1	+11.5	+14.5	+4.9/+3.7/+1.7	+3.2	+4.5
MoCo [26]	34.2	76.7	19.7	42.6	48.1/21.3/6.9	29.9	51.8
MoCo + CLD	43.1	80.4	25.4	50.0	53.1/24.9/9.4	33.3	57.3
vs. baseline	+8.9	+3.7	+5.7	+7.4	+5.0/+3.6/+2.5	+3.4	+5.5
<i>Supervised</i>							
CE	-	-	-	-	40.9/10.7/0.4	20.9	-
OLTR [40]	-	-	-	-	43.2/35.1/18.5	35.6	-

Table 1: CLD outperforms unsupervised baselines on **long-tailed datasets**, approaching supervised cross-entropy (CE) and OLTR [40]. The kNN (linear) classifiers are used for CIFAR (ImageNet-LT). CLD is significantly better than supervised CE on many-shot (100+), medium-shot ([20, 100]), few-shot (20—), and gets close to OLTR.

kNN accuracies	STL10	CIFAR10	CIFAR100	ImageNet100
DeepCluster	-	67.6	-	-
Exemplar [17]	79.3	76.5	-	-
Inv. Spread [63]	81.6	83.6	-	-
CMC [53]	-	-	-	79.2
NPID [58]	79.1	80.8	51.6	75.3
NPID + CLD	83.6	86.7	57.5	79.7
vs. baseline	+4.5	+5.9	+5.9	+3.6
MoCo [26]	80.8	82.1	53.1	76.6
MoCo + CLD	84.3	87.5	58.1	81.5
vs. baseline	+3.5	+5.4	+5.0	+4.9
BYOL [23]	-	-	-	75.8
BYOL + CLD	-	-	-	81.1
vs. baseline	-	-	-	+4.7

Table 2: **On self-supervised learning on small/medium-sized benchmarks:** STL10, CIFAR10, CIFAR100 and ImageNet-100, CLD delivers consistent gains as an add-on to various methods which use either standard contrastive loss (e.g. MoCo [26]) or without negative pairs (e.g. BYOL [23]). On ImageNet-100, we use our re-implemented code for baselines as they are better than those in CMC [53]. All baselines and their CLD add-on’s are optimized with the same training recipe for fair comparisons. For small- and medium-sized datasets, the nonlinear multi-layer perceptron (MLP) head performs worse than a linear projection head.

CIFAR100-LT. On ImageNet-LT, CLD outperforms NPID by 4.5% per top-5 accuracy, with the largest relative gain (24%) on few-shot classes; Our unsupervised CLD even significantly outperforms supervised plain Cross-Entropy (CE) by 8-14% and is catching up closely with supervised long-tail classifier OLTR (33.3% vs. 35.6%).

Results on major benchmarks. Table 2 shows that CLD outperforms SOTA on STL10, CIFAR10, CIFAR100 and ImageNet-100. On ImageNet, Table 3 shows that CLD consistently outperforms baselines under fair comparison settings: 200 training epochs, standard augmentations [58], and comparable model sizes. Adding CLD to InfoMin instead of MoCo produces 7.7% gain, by using an MLP projection



Figure 5: CLD top retrievals according to f_I (Columns 10-17) are less distracted by textures than NPID (Columns 2-9) for query images (Column 1) from the ImageNet validation set. Results are sorted by NPID’s performance. Correct retrievals, those in the same category as the query, are outlined in **green** and wrong ones in **red**. NPID seems more sensitive to textural appearance (e.g., Rows 1,4,5,7), first retrieve those with similar textures or colors.

head over feature $f(x)$, a cosine learning scheduler, extra data augmentation [8, 7, 54], and a Jigsaw branch as in PIRL [42]. Fig. A.11 shows CLD retrievals less distracted by textures.

Results on semi-supervised learning. Table 4 shows that CLD utilizes annotations far more efficiently, outperforming SOTA (InfoMin) by 6.1% with only 1% labeled samples. Baselines and CLDs follow OpenSelfSup benchmarks [69] for fair comparisons. Baseline results are copied from [69].

Transfer learning for object detection. We test the feature transferability by fine-tuning an ImageNet trained model for Pascal VOC object detection [18]. Table 5 shows that CLD not only outperforms its supervised learning counterpart by more than 6%(3%) in terms of AP in VOC07(VOC07+12), but also surpasses current SOTA of MoCo and MoCo v2.

4.2. Further Analysis

Why CLD performs better on long-tailed data? CLD groups similar samples and uses coarse-grained group prototypes instead of instance prototypes. There are two consequences. **1)** The positive to negative sample ratio is greatly increased from the instance branch to our group branch. For example, while each instance is compared against 4,096 negatives (as in MoCo), it is only compared against k negative centroids in our group branch, where $k \leq 256$ – our batch size. The importance of positives increases from $\frac{1}{4096}$ to $\frac{1}{k}$. CLD thus achieves better invariant mapping for all the classes, head or tail. However, the increased ratio is more important for tail classes, as they don’t have so many instances to rely on as head classes. **2)** The imbalance between head and tail classes in the negatives is also reduced in our group branch. While the distribution of instances in a random mini-batch is long-tailed, it would be more flattened across classes after clustering. The tail-class negatives would be better represented in the NCE loss. Fig. 6 shows that indeed

Methods	Architecture	#epoch	#GPU	top-1
NPID [58]	R50-Linear (24M)	200	8	56.5
w/ CLD	R50-Linear (24M)	200	8	60.6
MoCo [26]	R50-Linear (24M)	200	8	60.6
w/ CLD	R50-Linear (24M)	200	8	63.4
w/ CLD	R50-NormLinear (24M)	200	8	63.8
MoCo v2 [8]	R50-MLP (28M)	200	8	67.5
w/ CLD	R50-MLP (28M)	200	8	69.2
w/ CLD	R50-NormMLP (28M)	200	8	70.0
BYOL [†] [23]	R50-MLP (28M)	100	128	66.5
w/ CLD [‡]	R50-NormMLP (28M)	100	8	69.1
InfoMin [54]	R50-MLP (28M)	100	8	67.4
w/ CLD	R50-MLP (28M)	100	8	69.5
w/ CLD	R50-NormMLP (28M)	100	8	70.1
InfoMin [54]	R50-MLP (28M)	200	8	70.1
w/ CLD	R50-MLP (28M)	200	8	70.6
w/ CLD	R50-NormMLP (28M)	200	8	71.5
SimCLR [†] [7]	R50-MLP (28M)	100	128	66.5
SwAV [†] [6]	R50-MLP (28M)	100	128	66.5
BYOL [†] [23]	R50-MLP (28M)	100	128	66.5
SimSiam [†] [9]	R50-MLP (28M)	100	8	68.1
SimCLR [7]	R50-MLP (28M)	200	8	61.9
SimCLR [†] [7]	R50-MLP (28M)	200	128	68.3
SwAV [†] [6]	R50-MLP (28M)	200	128	69.1
BYOL [†] [23]	R50-MLP (28M)	200	128	70.6
MoCo v2 [8]	R50-MLP (28M)	200	8	67.5
SimSiam [†] [9]	R50-MLP (28M)	200	8	70.0
PIRL [42]	R50-Linear (24M)	800	32	63.6
CMC [53]	R50 _{L+ab} -Linear (47M)	280	8	64.1
CPC v2 [29]	R170-Linear (303M)	200	32	65.9
SimCLR [7]	R50-MLP (28M)	800	128	69.3
MoCo v2 [8]	R50-MLP (28M)	800	8	71.1
SwAV [6]	R50-MLP (28M)	400	128	70.1
SimSiam [†] [9]	R50-MLP (28M)	800	8	71.3

Table 3: **On self-supervised learning on ImageNet**, our CLD and NormMLP can be added to improve existing methods and achieve SOTA under 100-/200-epoch pre-training settings. Note that our experiments with CLD are conducted with 8 RTX 2080Ti GPUs, whereas PIRL, SimCLR, BYOL and SwAV require batch size 4,096 and 128/512 GPUs/TPUs for their original reported performance. All the results follow the standard linear evaluation protocol as used in [58, 26, 8, 54], except those marked by [†] (all copied from [9]): The linear classifier training of SwAV [6], BYOL [23] and SimSiam [9] uses base $lr = 0.02$ with a cosine decay scheduler, batch size 4096 with a LARS optimizer, giving these methods about 1% additional gain [9]. All the baseline results are from either their original papers or [9]. For BYOL+CLD results marked by [‡], the target network is updated once every 16 steps and uses batch size 256.

CLD has clearer class separation than MoCo.

How many groups shall CLD use? The ideal number of groups depends on the level of instance correlation, the number of classes, and the batch size. Table 7 shows that for CIFAR100, CLD is best when the number of groups is close to the number of classes, although CLD already outperforms MoCo at 10 groups. For ImageNet, the instance correlation is low; since the number of classes of 1,000 is larger than

Methods	Model	Label fraction	
		1%	10%
random initialization	ResNet50	1.6	21.8
rotation [21]	ResNet50	19.0	53.9
DeepCluster [4]	ResNet50	33.4	52.9
NPID [58]	ResNet50	28.0	57.2
MoCo [26]	ResNet50	33.2	60.1
SimCLR [7]	ResNet50	36.3	58.5
MoCo v2 [8]	ResNet50	38.7	61.6
InfoMin [†] [54]	ResNet50	39.7	62.3
MoCo v2 + CLD	ResNet50	44.4	63.6
InfoMin + CLD	ResNet50	45.8	64.4
vs. SOTA	ResNet50	+6.1	+2.1

Table 4: Top-1 accuracy of **semi-supervised learning** (1% and 10% label fractions) on ImageNet. CLD greatly improves SOTA. Baselines and CLD follow training recipes of OpenSelfSup benchmark [69] for fair comparisons, and apply the best performing hyper-parameter setting for each method. [†] denotes re-implemented results with [69].

Methods	VOC07		VOC07+12	
	AP ₅₀	AP	AP ₅₀	AP
supervised	74.6	42.4	81.3	53.5
JigSaw [22]	-	-	82.7	53.3
LocalAgg [71]	69.1	-	-	-
MoCo [26]	74.9	46.6	81.5	55.9
MoCo v2 [8]	-	-	82.0	56.4
SimCLR [7]	75.2	-	-	-
NPID + CLD	75.7	47.2	82.0	56.4
MoCo + CLD	76.8	48.3	82.4	56.7
MoCo v2 + CLD	77.6	49.3	82.7	57.0
InfoMin + CLD	77.9	49.8	83.0	57.2
vs. SOTA	+2.7	+3.2	+1.0	+0.8

Table 5: **Transfer learning** results on object detection: We fine-tune on Pascal VOC *trainval07+12* or *trainval07*, and test on VOC *test2007*. The detector is Faster R-CNN with ResNet50-C4. MoCo v2 model is pre-trained for 200 epochs. Note that our model outperforms SOTA methods without using an MLP head. Baseline results are copied from [26, 8].

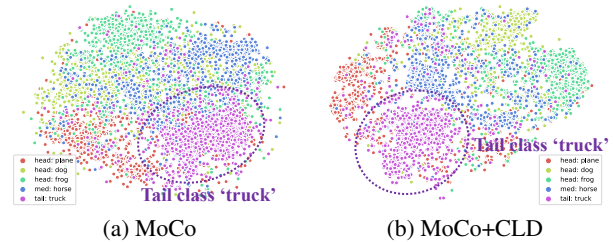


Figure 6: **t-SNE feature visualization** of (a) MoCo (b) MoCo + CLD on CIFAR10-LT. Tail class embedding is more compact and better separated from head classes. Head and medium-shot classes also have cleaner separation.

the batch size that our 8 GPUs can afford, we just choose the largest number of groups possible. We expect continuous gain with more groups and larger batches afforded by more GPUs. Nevertheless, our model wins with its merit of the CLD idea instead of a large compute.

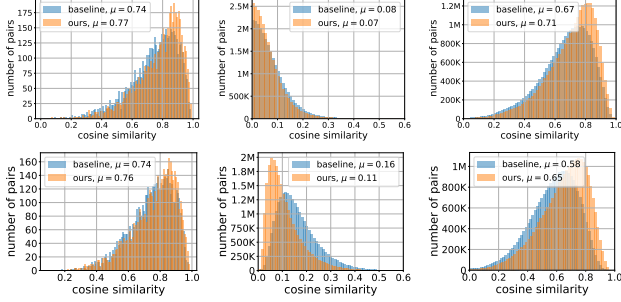
Similarity among positives / negatives? We measure fea-

CIFAR10	retrieval	NMI	kNN
NPID f_I	75.1	57.7	80.8
CLD f_I	78.6	63.5	86.7
f_G	75.6	69.0	81.4
CIFAR100			
NPID f_I	48.7	36.1	51.6
CLD f_I	50.2	43.8	57.5
f_G	48.8	49.4	51.8

Table 6: The **feature quality** of f_I and f_G evaluated by retrieval, normal-ized mutual information and kNN.

# groups	top-1
baseline	53.1
10	55.2
20	55.4
60	56.7
80	57.4
100	57.7
128	58.1

Table 7: **#groups vs. Accuracy** on CIFAR100 for CLD.



(a) pos pairs: A_{ii} (b) neg pairs: A_{ij} (c) difference: A_{ij}^{Δ}

Figure 7: CLD has more (dis)similar instances in positive(negative) pairs than baseline MoCo, creating a larger similarity gap. Columns 1-3 are the **histograms of cosine similarities** between positive and negative pairs and their differences per the linear projection layer for $f_I(x_i)$ (Row 1) and $f(x_i)$ (Row 2) on ImageNet100.

ture (cosine) similarity as $A_{ij}(f) \propto \frac{f(x_i)}{\|f(x_i)\|} \cdot \frac{f(x_j)}{\|f(x_j)\|}$, with A_{ii} ($A_{i,j \neq i}$) for positive (negative) pairs, and their gap is $A_{ij}^{\Delta} = A_{ii} - A_{ij}$. Fig. 7 shows that CLD has higher (lower) similarities between positives (negatives) than MoCo, creating larger gaps of A_{ij}^{Δ} , especially on $f(x_i)$ (Fig. 7 Row 2) – the common feature shared by our instance and group branches, making f a better discriminator than MoCo. It in turn improves f_I (Fig. 7 Row 1), the instance branch that runs parallel to the group branch f_G .

Mutual information characterization? We use kNN classification accuracy, Normalized Mutual Information (NMI), and retrieval accuracy R to compare features. $\text{NMI}(f, Y) = \frac{I(C|f, Y)}{\sqrt{H(C|f)H(Y)}}$ reflects global MI between feature f and downstream classification labels Y , where C is cluster labels predicted from k-Means clustering of f (k assuming the number of classes), $H(\cdot)$ is entropy, and $I(C|f; Y)$ is the MI between Y and C [51]. The top-1 retrieval accuracy $R(f, Y)$ reflects instance-level mutual information.

Table 6 shows that f_I is more accurate than f_G at retrievals and downstream classification. While f_G has higher NMI, its kNN accuracy is worse than f_I . That is, maximizing global MI would not deliver better downstream classification; maximizing instance-level MI is also important.

Unsupervised hyper-parameter tuning? Unsupervised

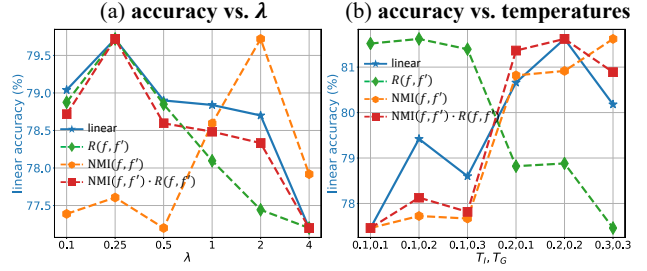


Figure 8: **Unsupervised hyper-parameter tuning** on ImageNet-100, for weight λ (left) and for the temperatures T_I, T_G used in CLD (right). Unsupervised evaluation metric $\text{NMI}(f, f') \cdot R(f, f')$ ranks models similarly as supervised linear classification, corroborating our idea that both global mutual information and augmentation-invariant local information are important for downstream performance. Each curve is individually normalized.

learning is meant to draw inference from unlabeled data. However, its hyper-parameters such as our weight λ and temperature T are often selected by labeled data in the downstream task. Self-supervised feature learning benchmarks pass as a supervised shallow feature learner with a few hyper-parameters. We explore unsupervised hyper-parameter selection based entirely on the unlabeled data.

We study how the supervised linear accuracy at the downstream can be indicated by unsupervised metrics such as NMI and R between feature $f(x)$ and $f' = f(x')$. Fig. 8 shows that the linear accuracy is well indicated by $R(f, f')$ for λ and by $\text{NMI}(f, f')$ for temperatures, but neither alone is sufficient. Their product $\text{NMI}(f, f') \cdot R(f, f')$ turns out to be a promising unsupervised evaluation metric.

5. Summary

We extend unsupervised learning to natural data with correlation and long-tail distributions by integrating local clustering into contrastive learning. It discovers between-instance similarity not by direct attraction and repulsion at the instance or group level, but cross-level between instances and groups. Their batch-wise and cross-view comparisons greatly improve the positive/negative sample ratio for achieving more invariant mapping. We also propose normalized projection heads and unsupervised hyper-parameter tuning.

Our extensive experimentation and analysis shows that CLD is a lean and powerful add-on to existing SOTA methods, delivering a significant performance boost on all the benchmarks and beating MoCo v2 and SimCLR on every reported performance with a much smaller compute.

Acknowledgments. This work was supported, in part, by Berkeley Deep Drive, US Government Fund through Etegent Technologies on Low-Shot Detection and Semi-supervised Detection, Texas Advanced Computing Center, and NTU NAP and A*STAR via Industry Alignment Fund.

References

- [1] Philip Bachman, R Devon Hjelm, and William Buchwalter. Learning representations by maximizing mutual information across views. In *NeurIPS*, 2019.
- [2] Elena Bernardis and Stella X. Yu. Finding dots: Segmentation as popping out regions from boundaries. In *CVPR*, 2010.
- [3] Christian Buchta, Martin Kober, Ingo Feinerer, and Kurt Hornik. Spherical k-means clustering. *Journal of Statistical Software*, 2012.
- [4] Mathilde Caron, Piotr Bojanowski, Armand Joulin, and Matthijs Douze. Deep clustering for unsupervised learning of visual features. In *ECCV*, 2018.
- [5] Mathilde Caron, Piotr Bojanowski, Julien Mairal, and Armand Joulin. Unsupervised pre-training of image features on non-curated data. In *ICCV*, 2019.
- [6] Mathilde Caron, Ishan Misra, Julien Mairal, Priya Goyal, Piotr Bojanowski, and Armand Joulin. Unsupervised learning of visual features by contrasting cluster assignments. *Advances in Neural Information Processing Systems*, 33, 2020.
- [7] Ting Chen, Simon Kornblith, Mohammad Norouzi, and Geoffrey Hinton. A simple framework for contrastive learning of visual representations. *arXiv preprint arXiv:2002.05709*, 2020.
- [8] Xinlei Chen, Haoqi Fan, Ross Girshick, and Kaiming He. Improved baselines with momentum contrastive learning. *arXiv preprint arXiv:2003.04297*, 2020.
- [9] Xinlei Chen and Kaiming He. Exploring simple siamese representation learning. *arXiv preprint arXiv:2011.10566*, 2020.
- [10] Adam Coates, Andrew Ng, and Honglak Lee. An analysis of single-layer networks in unsupervised feature learning. In *AISTATS*, 2011.
- [11] Fernando De la Torre and Takeo Kanade. Discriminative cluster analysis. In *ICML*, 2006.
- [12] Arthur P Dempster, Nan M Laird, and Donald B Rubin. Maximum likelihood from incomplete data via the em algorithm. *Journal of the Royal Statistical Society: Series B (Methodological)*, 1977.
- [13] Jia Deng, Wei Dong, Richard Socher, Li-Jia Li, Kai Li, and Li Fei-Fei. Imagenet: A large-scale hierarchical image database. In *CVPR*, pages 248–255, 2009.
- [14] Chris Ding and Tao Li. Adaptive dimension reduction using discriminant analysis and k-means clustering. In *ICML*, 2007.
- [15] Carl Doersch, Abhinav Gupta, and Alexei A Efros. Unsupervised visual representation learning by context prediction. In *ICCV*, 2015.
- [16] Jeff Donahue, Philipp Krähenbühl, and Trevor Darrell. Adversarial feature learning. In *ICLR*, 2017.
- [17] Alexey Dosovitskiy, Philipp Fischer, Jost Tobias Springenberg, Martin Riedmiller, and Thomas Brox. Discriminative unsupervised feature learning with exemplar convolutional neural networks. *TPAMI*, 2015.
- [18] Mark Everingham, Luc Van Gool, Christopher KI Williams, John Winn, and Andrew Zisserman. The pascal visual object classes (voc) challenge. *IJCV*, 88(2):303–338, 2010.
- [19] Guojun Gan, Chaoqun Ma, and Jianhong Wu. *Data clustering: theory, algorithms, and applications*. SIAM, 2007.
- [20] Georgios Georgakis, Md Alimoor Reza, Arsalan Mousavian, Phi-Hung Le, and Jana Koščeká. Multiview rgb-d dataset for object instance detection. In *3DV*, 2016.
- [21] Spyros Gidaris, Praveer Singh, Nikos Komodakis, et al. Unsupervised representation learning by predicting image rotations. In *ICLR*, 2018.
- [22] Priya Goyal, Dhruv Mahajan, Abhinav Gupta, and Ishan Misra. Scaling and benchmarking self-supervised visual representation learning. *arXiv preprint arXiv:1905.01235*, 2019.
- [23] Jean-Bastien Grill, Florian Strub, Florent Altché, Corentin Tallec, Pierre H Richemond, Elena Buchatskaya, Carl Doersch, Bernardo Avila Pires, Zhaohan Daniel Guo, Mohammad Gheshlaghi Azar, et al. Bootstrap your own latent: A new approach to self-supervised learning. *arXiv preprint arXiv:2006.07733*, 2020.
- [24] Michael U Gutmann and Aapo Hyvärinen. Noise-contrastive estimation of unnormalized statistical models, with applications to natural image statistics. *Journal of Machine Learning Research*, 2012.
- [25] Raia Hadsell, Sumit Chopra, and Yann LeCun. Dimensionality reduction by learning an invariant mapping. In *CVPR*, 2006.
- [26] Kaiming He, Haoqi Fan, Yuxin Wu, Saining Xie, and Ross Girshick. Momentum contrast for unsupervised visual representation learning. In *CVPR*, 2020.
- [27] Kaiming He, Georgia Gkioxari, Piotr Dollár, and Ross Girshick. Mask r-cnn. In *ICCV*, 2017.
- [28] Kaiming He, Xiangyu Zhang, Shaoqing Ren, and Jian Sun. Deep residual learning for image recognition. In *CVPR*, 2016.
- [29] Olivier J Hénaff, Aravind Srinivas, Jeffrey De Fauw, Ali Razavi, Carl Doersch, SM Eslami, and Aaron van den Oord. Data-efficient image recognition with contrastive predictive coding. *arXiv preprint arXiv:1905.09272*, 2019.
- [30] R Devon Hjelm, Alex Fedorov, Samuel Lavoie-Marchildon, Karan Grewal, Phil Bachman, Adam Trischler, and Yoshua Bengio. Learning deep representations by mutual information estimation and maximization. *arXiv preprint arXiv:1808.06670*, 2018.
- [31] Gao Huang, Zhuang Liu, Laurens Van Der Maaten, and Kilian Q Weinberger. Densely connected convolutional networks. In *CVPR*, 2017.
- [32] Jyh-Jing Hwang, Stella X. Yu, Jianbo Shi, Maxwell D Collins, Tien-Ju Yang, Xiao Zhang, and Liang-Chieh Chen. Segsort: Segmentation by discriminative sorting of segments. In *ICCV*, 2019.
- [33] Simon Jenni and Paolo Favaro. Self-supervised feature learning by learning to spot artifacts. In *CVPR*, 2018.
- [34] Xu Ji, João F. Henriques, and Andrea Vedaldi. Invariant information clustering for unsupervised image classification and segmentation. In *ICCV*, 2019.
- [35] Tapas Kanungo, David M Mount, Nathan S Netanyahu, Christine D Piatko, Ruth Silverman, and Angela Y Wu. An efficient k-means clustering algorithm: Analysis and implementation. *IEEE transactions on pattern analysis and machine intelligence*, 2002.
- [36] Alex Krizhevsky, Geoffrey Hinton, et al. Learning multiple layers of features from tiny images. *Citeseer*, 2009.

- [37] Alex Krizhevsky, Ilya Sutskever, and Geoffrey E Hinton. Imagenet classification with deep convolutional neural networks. In *NeurIPS*, 2012.
- [38] Gustav Larsson, Michael Maire, and Gregory Shakhnarovich. Colorization as a proxy task for visual understanding. In *CVPR*, 2017.
- [39] Junnan Li, Pan Zhou, Caiming Xiong, Richard Socher, and Steven CH Hoi. Prototypical contrastive learning of unsupervised representations. *arXiv preprint arXiv:2005.04966*, 2020.
- [40] Ziwei Liu, Zhongqi Miao, Xiaohang Zhan, Jiayun Wang, Boqing Gong, and Stella X Yu. Large-scale long-tailed recognition in an open world. In *CVPR*, 2019.
- [41] Michael Maire, Stella X. Yu, and Pietro Perona. Object detection and segmentation from joint embedding of parts and pixels. In *ICCV*, 2011.
- [42] Ishan Misra and Laurens van der Maaten. Self-supervised learning of pretext-invariant representations. *arXiv preprint arXiv:1912.01991*, 2019.
- [43] Feiping Nie, Zinan Zeng, Ivor W Tsang, Dong Xu, and Changshui Zhang. Spectral embedded clustering: A framework for in-sample and out-of-sample spectral clustering. *IEEE Transactions on Neural Networks*, 2011.
- [44] Mehdi Noroozi and Paolo Favaro. Unsupervised learning of visual representations by solving jigsaw puzzles. In *ECCV*, 2016.
- [45] Aaron van den Oord, Yazhe Li, and Oriol Vinyals. Representation learning with contrastive predictive coding. *arXiv preprint arXiv:1807.03748*, 2018.
- [46] Liam Paninski. Estimation of entropy and mutual information. *Neural computation*, 2003.
- [47] Deepak Pathak, Philipp Krahenbuhl, Jeff Donahue, Trevor Darrell, and Alexei A Efros. Context encoders: Feature learning by inpainting. In *CVPR*, 2016.
- [48] Chao Peng, Tete Xiao, Zeming Li, Yuning Jiang, Xiangyu Zhang, Kai Jia, Gang Yu, and Jian Sun. Megdet: A large mini-batch object detector. In *CVPR*, 2018.
- [49] Ben Poole, Sherjil Ozair, Aaron van den Oord, Alexander A Alemi, and George Tucker. On variational bounds of mutual information. *arXiv preprint arXiv:1905.06922*, 2019.
- [50] Jianbo Shi and Jitendra Malik. Normalized cuts and image segmentation. *IEEE Transactions on pattern analysis and machine intelligence*, 2000.
- [51] Alexander Strehl and Joydeep Ghosh. Cluster ensembles—a knowledge reuse framework for combining multiple partitions. *Journal of machine learning research*, 2002.
- [52] Fei Tian, Bin Gao, Qing Cui, Enhong Chen, and Tie-Yan Liu. Learning deep representations for graph clustering. In *AAAI*, 2014.
- [53] Yonglong Tian, Dilip Krishnan, and Phillip Isola. Contrastive multiview coding. *arXiv preprint arXiv:1906.05849*, 2019.
- [54] Yonglong Tian, Chen Sun, Ben Poole, Dilip Krishnan, Cordelia Schmid, and Phillip Isola. What makes for good views for contrastive learning. *arXiv preprint arXiv:2005.10243*, 2020.
- [55] Michael Tschannen, Josip Djolonga, Paul K Rubenstein, Sylvain Gelly, and Mario Lucic. On mutual information maximization for representation learning. *arXiv preprint arXiv:1907.13625*, 2019.
- [56] Laurens Van Der Maaten. Learning a parametric embedding by preserving local structure. In *Artificial Intelligence and Statistics*, 2009.
- [57] Ulrike Von Luxburg. A tutorial on spectral clustering. *Statistics and computing*, 2007.
- [58] Zhirong Wu, Yuanjun Xiong, Stella X Yu, and Dahua Lin. Unsupervised feature learning via non-parametric instance discrimination. In *CVPR*, 2018.
- [59] Junyuan Xie, Ross Girshick, and Ali Farhadi. Unsupervised deep embedding for clustering analysis. In *ICML*, 2016.
- [60] Jianwei Yang, Devi Parikh, and Dhruv Batra. Joint unsupervised learning of deep representations and image clusters. In *CVPR*, 2016.
- [61] Yi Yang, Dong Xu, Feiping Nie, Shuicheng Yan, and Yueting Zhuang. Image clustering using local discriminant models and global integration. *TIP*, 2010.
- [62] Jieping Ye, Zheng Zhao, and Mingrui Wu. Discriminative k-means for clustering. In *NIPS*, 2008.
- [63] Mang Ye, Xu Zhang, Pong C Yuen, and Shih-Fu Chang. Unsupervised embedding learning via invariant and spreading instance feature. In *CVPR*, 2019.
- [64] Stella X. Yu and Jianbo Shi. Segmentation with pairwise attraction and repulsion. In *ICCV*, 2001.
- [65] Stella X. Yu and Jianbo Shi. Understanding popout through repulsion. In *CVPR*, 2001.
- [66] Stella X. Yu and Jianbo Shi. Multiclass spectral clustering. In *CVPR*, 2003.
- [67] Xiaohua Zhai, Avital Oliver, Alexander Kolesnikov, and Lucas Beyer. S4L: Self-supervised semi-supervised learning. In *Proceedings of the IEEE international conference on computer vision*, pages 1476–1485, 2019.
- [68] Xiaohang Zhan, Xingang Pan, Ziwei Liu, Dahua Lin, and Chen Change Loy. Self-supervised learning via conditional motion propagation. In *CVPR*, 2019.
- [69] Xiaohang Zhan, Jiahao Xie, Ziwei Liu, Dahua Lin, and Chen Change Loy. OpenSelfSup: Open mmlab self-supervised learning toolbox and benchmark. 2020.
- [70] Richard Zhang, Phillip Isola, and Alexei A Efros. Colorful image colorization. In *ECCV*, 2016.
- [71] Chengxu Zhuang, Alex Lin Zhai, Daniel Yamins, et al. Local aggregation for unsupervised learning of visual embeddings. In *ICCV*, 2019.

6. Supplementary Materials

We provide further details on Kitchen-HC construction, implementation details, and various choices and experiments we have explored to validate our approach.

6.1. Kitchen-HC Dataset Construction

The original multi-view RGB-D kitchen dataset [20] is comprised of densely sampled views of several kitchen counter-top scenes with annotations in both 2D and 3D. The viewpoints of the scenes are densely sampled and objects in the scenes are annotated with bounding boxes and in the 3D point cloud. Kitchen-HC is constructed from multi-view RGB-D dataset Kitchen by extracting objects in their 2D bounding boxes. The customized Kitchen-HC dataset has 11 categories with highly correlated samples (from different viewing angles) and 20.8K / 4K / 14.4K instances for training / validation / testing. Fig. A.9 shows sample images in the original RGB-D Kitchen dataset from which our Kitchen-HC data are constructed (See samples used in Fig. 1).

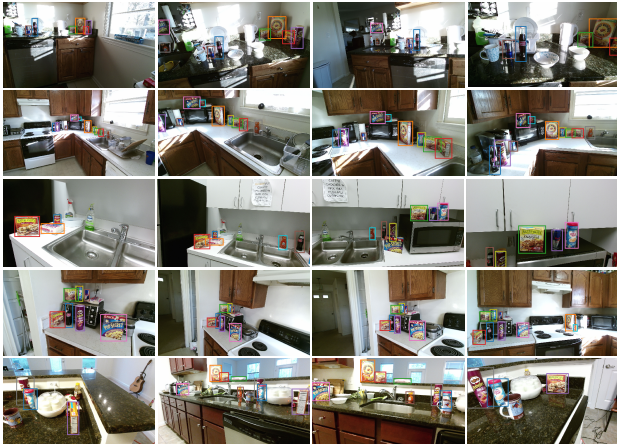


Figure A.9: Samples of multi-view RGB-D dataset Kitchen [20]. Instances of the same category captured from different perspectives are highly correlated. The high-correlation dataset Kitchen-HC is constructed from Kitchen by extracting objects in their bounding boxes.

6.2. Implementation Details

We use SGD as our optimizer, with weight decay 0.0001 and momentum 0.9. We follow MoCo and NPID [58, 26] and use only standard data augmentation methods for experiments on NPID+CLD and MoCo+CLD: random cropping, resizing, horizontal flipping, color and grayscale transformation, unless otherwise noticed.

1. **ImageNet-{100 [53], ILSVRC-2012 [13], Long-tail [40]}.** For ILSVRC-2012 and ImageNet-LT, we use mini-batch size 256, initial learning rate 0.03, on 8 RTX

2080Ti GPUs. For ImageNet-100, we use batch size 512 and a larger initial learning rate of 0.8 on 8 GPUs, and apply the same setting to baselines and our methods. Training images are randomly cropped and resized to 224×224 . For experiments on MoCov2+CLD with an MLP projection head, we extend the original augmentation in [26] by including the blur augmentation and apply cosine learning rate scheduler to further improve the performance on recognition as in [8]. BYOL+CLD is implemented based on OpenSelfSup [69] benchmark. For experiments on InfoMin+CLD and BYOL+CLD, we follow the same training recipe with InfoMin and BYOL [54, 23] for fair comparisons.

2. **CIFAR-{10, 100, 10-LT, 100-LT}, Kitchen-HC.** As [58], we use mini-batch size 256, initial learning rate 0.03 on 1 GPU for CIFAR [36] and Kitchen-HC. The number of epochs is 200 for CIFAR and 80 for Kitchen-HC. Training images are randomly cropped and resized to 32×32 .
3. **STL-10 [10].** Following [63], we use mini-batch size 256, initial learning rate 0.03, on 2 GPUs. Baseline models and baselines with CLD are trained on "train+unlabelled" split (105k samples), and tested on "test" split (5k samples). Training images are randomly cropped and resized to 96×96 .
4. **Transfer learning on object detection.** We use Faster R-CNN with a backbone of R50-C4, with tuned synchronized batch normalization layers [48] as the detector. As in [26], the detector is fine-tuned for 24k iterations for the experiment on Pascal VOC *trainval07+12* and 9k iterations for the experiment on Pascal VOC *trainval07*. The image scale is [480, 800] pixels during training and 800 at inference. NPID+CLD and MoCo+CLD use the same hyper-parameters as in MoCo [26]. The VOC-style evaluation metric [18] AP₅₀ at IoU threshold is 50% and COCO-style evaluation metric AP are used.
5. **Semi-supervised learning.** To make fair comparisons with baseline methods, we use OpenSelfSup [69] benchmark to implement baseline results and ours. We follow [67] and fine-tune the pre-trained model on two subsets for semi-supervised learning experiments, i.e. 1% and 10% of the labeled ImageNet-1k training datasets in a class-balanced way. The necks or heads are removed and only the backbone CNN is evaluated by appending a linear classification head.

We apply greedy search on a list of hyper-parameter settings with the base learning rate from {0.001, 0.01, 0.1} and the learning rate multiplier for the head from {1, 10, 100}. We choose the optimal hyper-parameter

setting for each method. Empirically, all baselines and their alternatives with CLD obtain the best performance with a learning rate of 0.01 and a learning rate multiplier for the head of 100. We train the network for 20 epochs using SGD with weight decay 0.0001 and a momentum of 0.9, and a mini-batch of 256 on 4 GPUs. The learning rate is decayed by 5 times at epoch 12 and 16 respectively.

6.3. Which Clustering Method to Use?

We have tried two popular clustering methods: k-Means clustering and spectral clustering, both implemented in Pytorch for fast performance on GPUs.

k-Means clustering [3, 35] aims to partition n representations into k groups, each representation belongs to the cluster with the nearest cluster centroid, serving as a prototype of the cluster. We use spherical k-Means clustering which minimizes: $\sum (1 - \cos(f_i, u_{c(i)}))$ over all assignments c of objects i to cluster ids $c(i) \in \{1, \dots, k\}$ and over all prototypes u_1, \dots, u_k in the same feature space as the feature vector f_i representing the objects. We use binary cluster assignment, where the cluster membership $m_{ij} = 1$ if item i is assigned to cluster j and 0 otherwise. The following k-means objective can be solved using the standard Expectation-Maximization algorithm [12]:

$$\begin{aligned} \Phi(M, \{u_1, \dots, u_C\}) &= \sum_{i,j} m_{ij} (1 - \cos(f_i, u_{c(i)})) \\ &= \sum_{i,j} m_{ij} (1 - \frac{f_i \cdot u_{c(i)}}{\|f_i\| \cdot \|u_{c(i)}\|}). \end{aligned} \quad (4)$$

Spectral clustering [50, 66] treats data points as nodes of a graph.

1. For feature $f_i \in \mathbb{R}^{d \times 1}$ of N samples, we build a weighted graph $\mathbf{G} = (\mathbf{V}, \mathbf{E})$, with weight measuring pairwise feature similarity: $w_{i,j} = \frac{f_i \cdot f_j}{\|f_i\| \cdot \|f_j\|}$.
2. Let \mathbf{D} be the $N \times N$ diagonal degree matrix with $d_{ij} = \sum_{j=1}^n w_{ij}$ and \mathbf{L} be the normalized Laplacian matrix:

$$\mathbf{L} = \mathbf{D}^{-\frac{1}{2}} (\mathbf{D} - \mathbf{W}) \mathbf{D}^{-\frac{1}{2}} \quad (5)$$

3. We compute the k largest eigenvalues of \mathbf{L} and use the corresponding k row-normalized eigenvectors E_i as the globalized new feature [50, 66]. We apply EM to find the cluster centroids.

Table A.8 shows that k-means clustering achieves better performance on Kitchen-HC and outperforms optimal spectral clustering result by 1.8% when the group number is 10. However, as the group number increases, the performance difference becomes negligible.

group	spectral	k-Means
10	77.1%	78.9%
64	74.5%	76.3%
128	72.6%	73.4%
256	70.5%	70.8%

Table A.8: Top-1 kNN accuracies on Kitchen-HC under different group numbers for different clustering methods.

NPID+CLD	Subspace	Cross-augmentation	CIFAR-10	CIFAR-100
✗			80.8%	51.6%
✓	share		82.7%	53.3%
✓	separate		84.2%	55.0%
✓	separate	✓	86.5%	57.5%

Table A.9: Ablation study on various components of our method, i.e. adding the cross-level discrimination, projecting the representation to two different spaces, and using cross-augmentation comparison between x_i and x'_i . kNN top-1 accuracy is reported here.

6.4. Are Separate Feature and Group Branches Necessary?

Intuitively, instance grouping and instance discrimination are at odds with each other. Our solution is to formulate the feature learning on a common representation, forking off two branches where we can impose grouping and discrimination separately. Table A.9 shows that projecting the representation to different spaces and jointly optimize the two losses increase top-1 kNN accuracy by 1.5% and 1.8% on CIFAR-10 and CIFAR-100 respectively.

6.5. How Effective Is Cross-Augmentation Comparisons?

Instance-level discrimination presumes each instance is its own class and any other instance is a negative. The groups needed for any group-level discrimination have to be built upon local clustering results extracted from the current feature in training, which are fluid and unreliable.

Our solution is to seek the most certainty among all the uncertainties: We presume stable grouping between one instance and its augmented version, and our cross-level discrimination compares the former with the groups derived from the latter. We roll the three processes: instance grouping, invariant mapping, and instance-group discrimination all into one CLD loss.

Table A.9 shows that our cross-augmentation comparison increases the top-1 accuracy by more than 2% on recognition task. It demands the feature not only to be invariant to data augmentation, but also to be respectful of natural grouping between individual instances, often aligning better with downstream semantic classification.

6.6. How Sensitive Are Hyper-parameters Weight λ and Temperature T ?

λ controls the relative importance of CLD with respect to instance-level discrimination, and helps strike a balance between the caveates of noisy initial grouping and the benefits it brings with coarse-grained repulsion between instances and local groups. Table A.10 shows that, at a fixed group number, $\lambda = 0.25$ achieves optimal performance, and a larger λ generally leads to worse performance and even decreases top-1 accuracy by 3.1% at $\lambda = 3$.

	NPID+CLD		MoCo+CLD	
	top-1 (%)	top-5 (%)	top-1 (%)	top-5 (%)
$\lambda = 0$	75.3	92.4	77.6	93.8
$\lambda = 0.1$	78.8	94.4	80.3	95.0
$\lambda = 0.25$	79.7	95.1	81.7	95.7
$\lambda = 0.50$	78.9	94.4	80.5	95.2
$\lambda = 1.0$	78.8	94.5	80.1	94.8
$\lambda = 3.0$	76.6	93.2	78.4	94.1

Table A.10: Top-1 and top-5 linear classification accuracies (%) on ImageNet-100 with different λ 's. The backbone network is ResNet-50.

T is known to be critical for discriminative learning and can be sometimes tricky to choose. Table A.11 shows that the best performance is achieved at $T = 0.2$ for both CIFAR and ImageNet-100. With local grouping built into our CLD method, we find the sensitivity of T is greatly reduced.

$T(T_I = T_G)$	0.07	0.1	0.2	0.3	0.4	0.5
CIFAR-100	57.9%	57.8%	58.1%	58.1%	57.6%	57.2%
ImageNet-100	79.3%	79.6%	81.7%	80.7%	79.4%	79.0%

Table A.11: Linear (ImageNet-100) and kNN (CIFAR-100) evaluations for models trained with different choices of temperature T , $T_I = T_G$ for simplicity.

6.7. Is A Larger Memory Bank Always Better for Discriminative Learning?

A larger memory bank includes more negatives and is known to deliver a better discriminator. However, we cannot simply adjust the memory bank size according to NMI or retrieval accuracy in order to deliver the best performance on downstream classification.

Fig. A.10 compares NMI and retrieval accuracies under different negative prototype numbers. If there are too many negatives, the model would focus on repelling negative instances, ignoring the commonality between instances; if there are too few negatives, the model would be subject to random fluctuations from batch to batch, affecting optimization and convergence. However, neither the number of negatives (i.e. infoNCE-k) to obtain the best retrieval accuracy nor the number of negatives to achieve the best NMI score can deliver the best downstream classification task. To

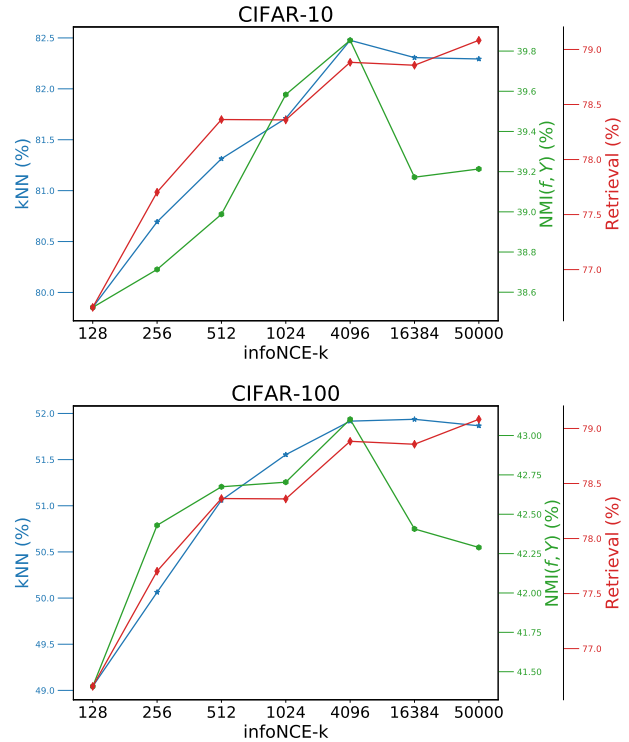


Figure A.10: MoCo trained with different memory bank sizes are evaluated with NMI, retrieval and kNN accuracy. While a larger memory bank improves the retrieval performance, the classification accuracy and NMI score do not always increase: the NMI score drops sharply due to a large negative/positive ratio. There is a trade-off for best performance at downstream classification.

deliver optimal performance at downstream classification task, there is a trade-off between local mutual information (evaluated by retrieval task) and global mutual information (evaluated by Normalized Mutual Information).

6.8. Sample Retrievals

Fig. A.11 shows our near-perfect sample retrievals on ImageNet-100 using $f_I(x)$ in our NPID + CLD model. On the contrary, NPID seems to be much more sensitive to textural appearance (e.g., Rows 1,4,6,7), first retrieve those with similar textures or colors. CLD is able to retrieve semantically similar samples. Our conjecture is that by gathering similar textures into groups, CLD can actually find more informative feature that contrasts between groups. For example, the 5th query image is a Chocolate sauce, which has similar texture with Grouper fish. NPID incorrectly retrieves many images from the Grouper Fish class, but CLD successfully captures the semantic information of the query image, and retrieves instances with the same semantic information.

